land

MDPI

Article

Clarification of the Boundaries of Lands of Historical and Cultural Heritage and Determination of Their Protection Zones by Remote Sensing Methods

Borys Chetverikov [1,*], Volodymyr Hlotov [1] and Krzysztof Bakuła [2]

[1] Department of Photogrammetry and Geoinformatics, Institute of Geodesy, Lviv Polytechnic National University, S.Bandery Str., 79013 Lviv, Ukraine; volodymyr.m.hlotov@lpnu.ua
[2] Department of Photogrammetry, Remote Sensing and Spatial Information Systems, Faculty of Geodesy and Cartography, Warsaw University of Technology, Pl. Politechniki 1, 00-661 Warsaw, Poland; krzysztof.bakula@pw.edu.pl
* Correspondence: borys.v.chetverikov@lpnu.ua; Tel.: +380-631671585

Abstract: Determining precise boundaries and protective zones for historical and cultural objects enables their effective preservation. This article presents the framework for establishing protective zones around historical and cultural heritage sites existing in Ukraine, using the example of the Citadel defensive complex located in Lviv (Ukraine). It proposes general and detailed conceptual models for the combined application of remote and non-invasive methods for investigating historical and cultural heritage sites. It introduces the theory of integrating radar satellite imaging with ground-based georadar imaging. Additionally, it presents a software module that has been developed to analyze collected data on two-dimensional historical and cultural heritage objects, refine their boundaries, and establish protective zones around them. The result of the work is the determination of extremum points of vertical displacement on the territory of the historical and cultural heritage site "Lviv Citadel" in Ukraine using SAR, and the construction of a map of vertical displacements. A classification of these points was carried out, after which two of them were investigated using GPR for anomalies. Artifacts from World War II were discovered at each of these points. Using the developed software module, updated boundaries of the site were constructed, taking into account the underground artifacts and protective zones.

Keywords: remote sensing; GPR; non-invasive methods; historical and cultural heritage object; protective zone; boundary refinement; software module

check for updates

Citation: Chetverikov, B.; Hlotov, V.; Bakuła, K. Clarification of the Boundaries of Lands of Historical and Cultural Heritage and Determination of Their Protection Zones by Remote Sensing Methods. *Land* **2024**, *13*, 923. https://doi.org/10.3390/land13070923

Academic Editor: Deodato Tapete

Received: 5 May 2024
Revised: 20 June 2024
Accepted: 22 June 2024
Published: 25 June 2024

Copyright: © 2024 by the authors. Licensee MDPI, Basel, Switzerland. This article is an open access article distributed under the terms and conditions of the Creative Commons Attribution (CC BY) license (https://creativecommons.org/licenses/by/4.0/).

1. Introduction

The preservation of immovable objects of historical and cultural heritage is imperative for maintaining a connection with our past, fostering cultural identity, and enriching the collective human experience. However, the challenges associated with demarcating accurate boundaries and establishing protective zones demand innovative solutions. Traditional methods often fall short of providing the necessary precision and comprehensive understanding of the site's dynamics. Remote investigation methods, such as satellite imaging and aerial surveys, present a promising avenue for overcoming these challenges. The contemporary relevance of refining boundaries and determining protective zones lies in the potential to harmonize cultural conservation with technological advancements, ensuring the sustainable protection of our invaluable heritage for future generations [1–5].

The issue of refining boundaries and determining protective zones for historical and cultural heritage sites using remote sensing methods has several aspects. The use of remote methods, such as satellite imaging or aerial photography, may be limited in the accuracy of geospatial data. This can lead to inaccuracies in refining object boundaries and determining protective zones. Collecting and analyzing data from various sources, such as geodetic

measurements, historical documents, archaeological research, etc., requires the integration of diverse information [6,7]. The complexity of coordinating and analyzing these data can be a challenge. Determining protective zones and refining boundaries are subject to regulation and legislation. Problems may arise due to ambiguity in legislation, discrepancies in interpretation, or insufficient clarity regarding specific rules and standards [8–15]. The processes of refining boundaries and determining protective zones may provoke public dissatisfaction, especially when it concerns residential buildings or businesses. The degree of community involvement in decision-making and discussion of heritage conservation measures plays a significant role. The use of geographic information systems and new technologies, such as artificial intelligence may pose technical challenges, such as staff training, maintaining technical infrastructure, and ensuring data security. Historical and cultural objects may change over time. Management systems must be flexible and adaptable to changes in the environment and conditions. Addressing these issues requires a comprehensive approach, including close collaboration among surveying specialists, historians, archaeologists, community representatives, and legislators [16–21].

In recent years, Ukraine has faced challenges in accounting for planar immovable objects of historical and cultural heritage, especially those with partially or fully destroyed above-ground parts. Many such objects are privately owned or partially border private parcels of land. As a result, many of these objects have been subject to legal proceedings over boundaries and protective zones. In response, authorities have decided to temporarily register objects in point form as centroids of polygons, with protective zones measured from the centroid rather than the historical boundaries of the object. This approach allows for the registration of all historical and cultural heritage objects, followed by the establishment and adjustment of historical boundaries. This approach has both positive aspects and drawbacks, as the protective zone from the centroid may not always cover the entire territory of the object, especially if it has an irregular shape (Figure 1). The protective zone of a historical and cultural heritage object is set at 300 m from the polygon centroid in undeveloped areas and may be reduced depending on the surrounding development through contractual agreements.

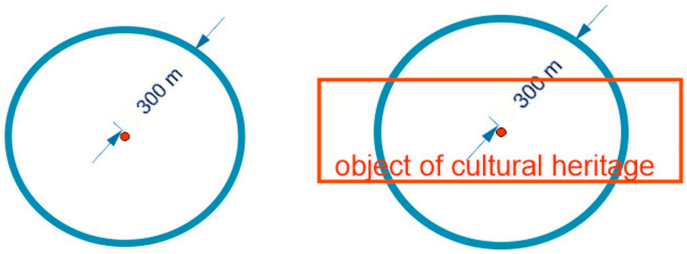


Figure 1. Buffer zones constructed around the centroid of the object and around the centroid of irregularly shaped polygons.

2. Materials and Methods

The aim of this study is to propose a conceptual model for refining the boundaries of historical and cultural heritage objects using remote and non-invasive methods. To achieve this goal, the Citadel defensive complex located in Lviv, Ukraine, and listed among the objects of national significance in terms of historical and cultural heritage, was chosen as the research polygon.

Let's consider existing scientific research on the combination of SAR and GPR methods. Gleich [22] investigates how Synthetic Aperture Radar (SAR) and Ground-Penetrating Radar (GPR) can be used to identify wet zones in a hydroelectric power station channel, focusing on the integration of these methods to enhance detection accuracy. Zych [23] explores methods to improve the resolution of GPR images through targeted SAR processing, highlighting techniques for obtaining clearer and more detailed subsurface images. Mostafa et al. [24] study SAR processing methods for detecting buried objects using GPR. Notteber et al. [25] investigate the enhancement of soil moisture estimation based on SAR

images using GPR data. These studies are empirical in nature [26]. In our research, we present a concept of heterogeneous data processing, which culminates in the creation of a specialized software module for processing data obtained from SAR and GPR.

2.1. Information about the Research Object

Lviv Citadel is a fortification structure in the Halytskyi district of Lviv. The Citadel was built between 1852 and 1854 and consists (according to the original plan) of four round towers and a V-shaped barracks building. All the round towers were artillery towers and were constructed according to the system proposed by Austrian General Maximilian-Joseph d'Este (these structures replaced traditional bastions and were named Maximilian towers).

During World War I, the Austrians decided not to defend Lviv and surrendered it without a fight to the Russian army. In 1914–1915, the Citadel housed a Russian garrison.

During the Ukrainian–Polish War in early November 1918, the Citadel was occupied by a Ukrainian garrison. To capture the Citadel, the Poles organized a special combat group called "Citadel". The main Polish assault was directed at the southern tower. After several weeks of fighting, on the night of November 20–21, this tower was taken. Since then, it has remained partially destroyed. Periodically, historical reenactments of the Polish attack on the Citadel are held near its walls.

During World War II (1941–1944), the Germans set up a prisoner-of-war camp (Stalag-328 "Tsutadell") on the Citadel's grounds. At the same time, soldiers were stationed there, and there were military barracks. This grim episode during the war lasted for three years. After the camp's decentralization, only the military barracks remained on most of the territory.

In Figure 2, the geographical location of the Citadel is shown in the context of the borders of Ukraine and the city of Lviv.



Figure 2. Schematic location of the research area of the Lviv Citadel.

2.2. Description of the Developed Conceptual Research Model

We have developed and proposed a generalized and detailed conceptual model for conducting our research (Figure 3).

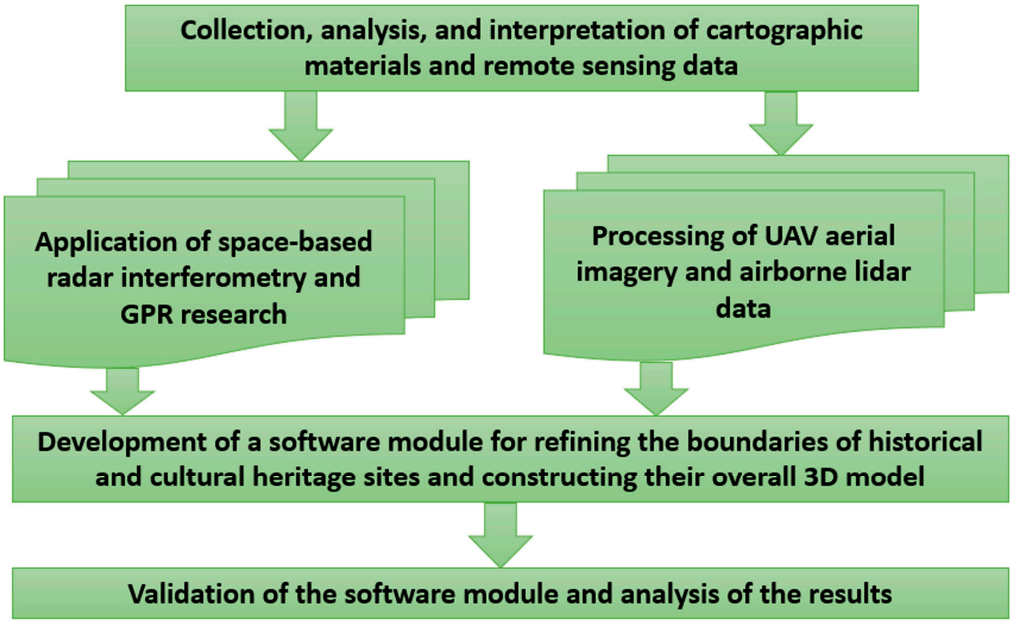


Figure 3. The conceptual model for using remote sensing and ground-penetrating radar data to study historical and cultural heritage land.

The generalized conceptual model comprises six main blocks, starting from data collection from remote sensing and ground-penetrating radar imaging and ending with the final analysis and interpretation of the acquired data. Additionally, the generalized conceptual model includes data processing and visualization. At this stage, satellite imagery is processed to obtain detailed information about land covers, and ground-penetrating radar data are processed to detect underground structures such as building foundations or archaeological remains. Visualization of processed data aids in better understanding the geographic context of the studied area. In the preliminary analysis and data interpretation block, machine learning algorithms and computer vision are employed to classify land covers and identify features related to historical and cultural objects. Interpretation of the analysis results aims to identify lands of historical and cultural significance, such as the locations of ancient settlements, fortresses, or archaeological sites. The data validation stage occurs after image classification, when it is essential to validate the results. This involves comparing classified data with a validation dataset containing information about known historical and cultural objects. Validation helps assess the accuracy and reliability of the classification and identify potential errors. After validation, ground investigations are recommended for a detailed study of historical and cultural objects. This may include visiting locations where potential objects are detected, gathering additional information, archaeological excavations, or ground-penetrating radar profiles to obtain more detailed data on the structure and characteristics of objects. The next step involves creating maps depicting lands of historical and cultural significance based on classified data and the results of ground investigations. This can be done by generating vector or raster layers showing the locations and types of historically and culturally significant objects on the map. The final stage involves the analysis and interpretation of the obtained results. This may include identifying patterns, relationships, and trends in the distribution of lands of historical and cultural significance, as well as establishing the significance and status of the identified objects [27–29].

The detailed conceptual model provides a thorough description of each research stage. It includes the collection, analysis, and interpretation of cartographic materials and remote

sensing data, followed by branching into parallel processes of processing spaceborne radar images and obtaining interferograms, as well as obtaining orthophotos and point clouds from aerial imagery and UAV Lidar data (although in this research example we focus only on radar interferometry and ground-penetrating radar imaging, the conceptual model describes the application of various remote and non-invasive research methods for a comprehensive study of historical and cultural heritage objects). The block of processing spaceborne radar images and obtaining interferograms is further divided into manual and semi-automatic result retrieval. Subsequently, a software module is developed for loading resulting data and constructing overall 3D models of surface and subsurface elements of historical and cultural heritage objects. After analyzing the acquired data, the overall research model of immovable historical and cultural heritage objects is constructed, followed by the semi-automatic establishment of protective zones for historical and cultural heritage objects based on the obtained data [30–32].

The technology for implementing the conceptual model involves using two types of input data: analysis of archival aerial photographs (such as those from the World War II era), if the object of study is, for example, mass graves or similar objects that are often not depicted on cartographic materials, and analysis of archival cartographic materials (cadastral maps, other cartographic products) for other planar objects of historical and cultural heritage. After analyzing archival aerial photographs, they are interpreted through visual inspection by the performer or by computer vision to identify potential areas of interest, such as possible locations of mass graves and other elements of historical and cultural heritage objects. If areas of interest are identified at this stage, the transition to ground-penetrating radar surveys to detect anomalies occurs; otherwise, areas of interest are determined, and the search for medium- or high-resolution satellite radar images begins, which are processed using radar interferometry methods in SNAP or SARScape software packages, or others. Interferograms are obtained, extreme points of vertical displacement are determined, and maps of vertical displacement are constructed. Then, ground-penetrating radar surveys are carried out to detect anomalies. The transition to ground-penetrating radar imaging also occurs after localizing objects of historical and cultural heritage and monitoring changes in their boundaries using various cartographic materials over time. If ground-penetrating radar surveys yield no results, the research is discontinued; if anomalies are found, their interpretation and identification of elements of historical and cultural heritage objects occur. In parallel with these processes, software development for semi-automatic searches of areas of interest in ground-penetrating radar imaging and construction of a general 3D model using Visual Basic or Python programming languages, as well as aerial lidar and UAV aerial imagery, are carried out. Point clouds are processed to create orthophoto plans, and digital surface models or digital terrain models are built and compared, depending on the object. Interpreted anomalies from ground-penetrating radar surveys and digital surface models or digital terrain models from UAVs are uploaded into the developed software module, which involves data loading and construction of 3D models of surface and subsurface elements of the historical and cultural heritage objects, as well as analysis and interpretation of elements for inclusion of newly discovered details within the defined boundaries of the historical and cultural heritage objects. If the elements fall within the recognized boundaries of the object, the research is completed; if not, the boundaries of the historical and cultural heritage objects are refined, and recommendations for establishing protective zones are proposed.

The primary focus of this research was on spaceborne synthetic aperture radar (SAR) and ground-penetrating radar (GPR) imaging methods.

2.3. Study of the Lviv Citadel Territory Using the SAR Method

As input data for SAR analysis, 36 satellite images obtained from the Sentinel-1 satellite over two years from 2020 to 2022 were utilized. The image resolution is 10 × 10 m for the IW.

Satellite radar images were processed using ENVI SARscape software. These images were obtained in the C-band with VV + VH polarization and in interferometric wide swath (IW) mode. In this case, the swath of each image is 250 km.

Sentinel-1A images are available in three processing levels: Level-0, Level-1, Level-2. Our input data are in the first processing level. Level-1 data are publicly available products designed for most data users. Level-1 products are produced as Single Look Complex (SLC) and Ground Range Detected (GRD). The images were obtained from the Copernicus geospatial portal.

Radar data were processed using ENVI SARscape software. For the SBAS method, the cycle of interferometric processing in ENVI SARscape is performed for each pair of images in the interferometric series. Image pairs are automatically selected from the downloaded series of images. The first step of interferometric processing is precise spatial alignment (coregistration) of the master and slave radar images in the interferometric series, which is performed in the SARscape module in automatic mode. At this stage, the coregistration accuracy is achieved to one or several pixels; at the second stage, there is a subpixel accuracy of coregistration; and at the third stage, accuracy is to 1/100 pixels. The next step calculates complex interferograms, which are the result of complex element-wise multiplication of phase of radar image pairs in the interferometric series. The complex interferogram contains several components: topographic phase, deformation phase, atmospheric phase, and electromagnetic noise. Complex element-wise multiplication of phases is necessary for each pair of images in the interferometric series. The main output file of this procedure is the differential interferogram, which is the result of subtracting the synthesized relief phase from the complex interferogram. The differential interferogram contains the component of surface deformation that occurred between acquisitions, the phase noise component, and the component of atmospheric conditions influence during each image acquisition in the selected series. Adaptive filtering of the differential interferogram was used to reduce noise using the Goldstein filter for each pair of images (Figure 4).

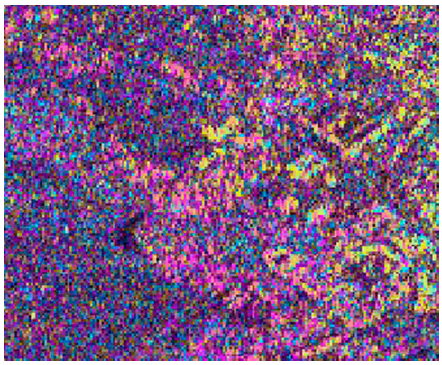


Figure 4. Filtered differential interferogram using the Goldstein filter.

After filtering the phase noise (Goldstein algorithm), a reduction in the size of noise areas and an increase in the radius of noise correlation can be observed. To obtain a continuous phase, i.e., to remove phase jumps by 2π, it is necessary to perform the phase unwrapping procedure for each pair of images. There are about a dozen algorithms for performing the phase unwrapping operation, each with its own advantages and disadvantages. Phase unwrapping was performed using the Minimum Cost Flow method with Delaunay triangulation. In this method, the gradient of the unwrapped phase is restored by changing the integer number of phase periods of individual pixels. To separate significant phase values from insignificant ones, the coherence of the phase (phase correlation) was used as an auxiliary parameter. It is measured in dimensionless quantities from 0 to 1 and is calculated using the filtered differential interferogram. Further, the so-called inversion was performed, which restores the temporal dynamics of displacements from cross-temporal pairs of images. After that, the results were geocoded and converted to vector format.

2.4. Study of Extremum Points of Vertical Displacement Using the GPR Method

After determining the points of maximum surface displacement using radar interferometry, we proceeded with ground-based non-invasive investigations using ground-penetrating radar (GPR). Seven points were processed, which raised the most questions, and were located either on the boundary of the historical and cultural heritage object or beyond it. Anomalies of artifacts were deciphered on the radargrams at two points (Figure 5), one located on the current territory of the tennis court, and the other beyond the boundary of the current object.

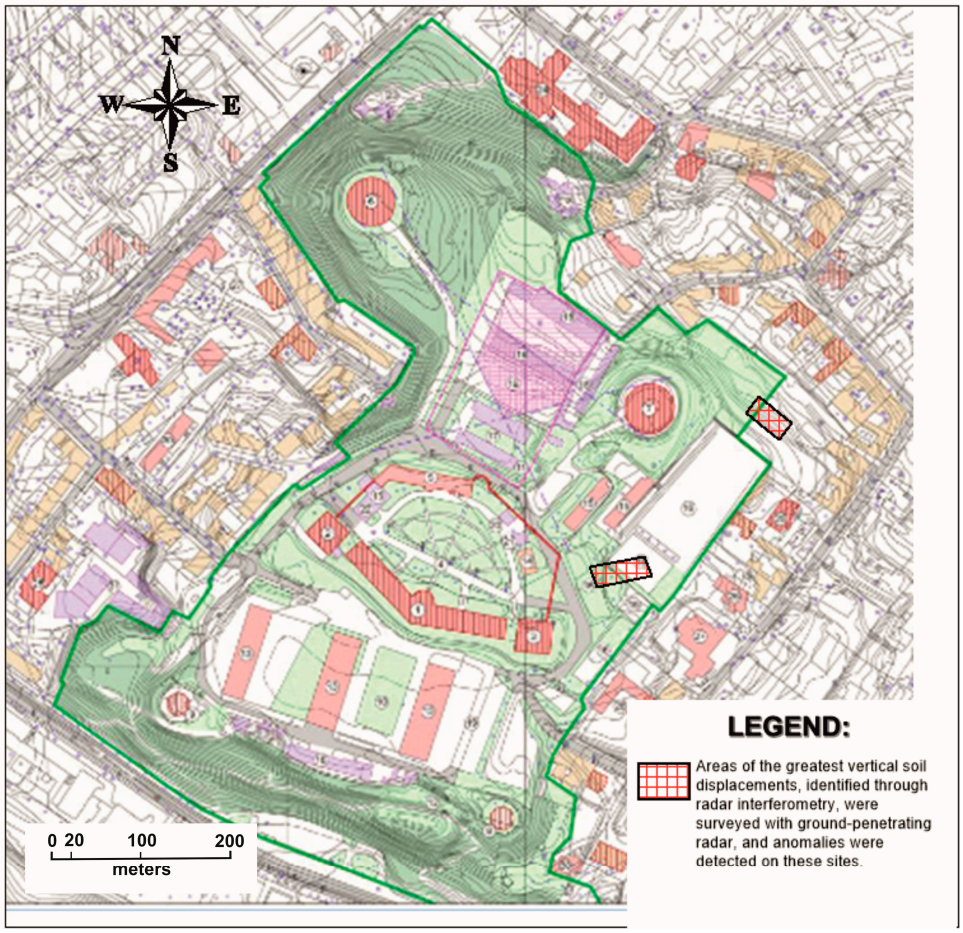


Figure 5. Areas surveyed with GPR (AOI1—lower area, AOI2—upper area) where anomalies were identified.

Ground-penetrating radar imaging was conducted at points of extreme vertical displacement of the Earth's surface, obtained from interferograms. Ground-penetrating radar imaging was performed using the UTSI GV3_1 GPR system (Figure 6). The main characteristics of this system are provided in Table 1.

Table 1. The main technical specifications of the UTSI GV3_1 GPR (Ground-Penetrating Radar).

The Name of the Characteristic	Parameter
Antenna frequency	400 Hz
Data reading interval	0.15
Transverse step	0.15 m.

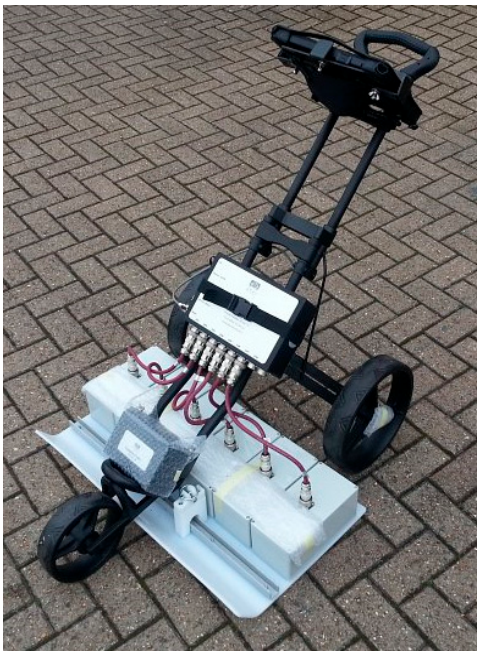


Figure 6. Sensor used—UTSI GV3_1 GPR.

The ground-penetrating radar (GPR) emits high-frequency pulses from the transmitting antenna directly into the ground. When these electromagnetic waves pass through gaps in the soil or solid objects, a portion of this energy is reflected back to the receiving antenna, while another portion continues further and may be reflected from deeper fractures in the ground. This process continues until the energy of the transmitted wave decreases to a level that does not allow further penetration. By measuring the time of the reflected wave's return, the depth of the object can be determined along the vertical plane. Data from multiple planes are processed further to reflect the plan of the surveyed area at the desired depth.

The ability of soil to transmit radio waves depends on several factors, including soil conductivity, dielectric permittivity, moisture content, density, porosity, temperature, physical structure, the frequency used, and the amount of salts present in the soil. The most important factor is soil conductivity, which determines the wave propagation speed and penetration depth. Soils with high conductivity lead to signal loss. Overall, the soils in the Lviv region are suitable for GPR. The type and condition of the soils in the studied area are loose, homogeneous, well-fractionated sandy loams with fine gravel.

Dielectric permittivity and soil moisture significantly affect GPR surveys. Dielectric permittivity influences the speed of radio wave propagation through the soil, altering their sensitivity to various objects and structures within the soil. Moisture also impacts this process, as wet soils can reflect radio waves and create artifacts in the images. These factors must be considered when interpreting GPR data to achieve more accurate results.

The surface cover consists of 85–95% grassy/herbaceous vegetation with shrubs and 10–25% trees with well-developed crowns on the northern and eastern sides of the surveyed area.

2.5. Integration of SAR and GPR Research Results and Development of a Software Module for Automatic Boundary Correction of the Object and Its Protective Zone

To combine the results of spaceborne radar interferometry from the Sentinel-1 satellite and GPR imaging at a specific point, a weighted approach can be utilized (1).

$$R = \alpha \cdot C_i + \beta \cdot C_g \quad (1)$$

where:

R is the result of combining the two methods for a specific point on the surface.
α and β are weights that determine the importance of each data source in the combined result. These weights can be determined by experts or through optimization depending on the specific application.
C_i is the measurement result obtained from spaceborne radar interferometry at a specific point.
C_g is the result of ground-penetrating radar imaging at the same point.

This approach allows combining information from both sources to obtain a more complete and reliable representation of a specific point.

The formula for combining InSAR (Interferometric Synthetic Aperture Radar) and GPR (Ground-Penetrating Radar) can be complex and depends on specific use cases. However, the general idea is to integrate information obtained from both sources to improve the accuracy of interpreting and analyzing geological structures or soil properties.

A possible general Formula (2) could be as follows:

$$Result = f(INSAR_data, GPR_data) \quad (2)$$

Here, f is a function that may include various data processing operations, filtering, and other analysis methods to achieve a more accurate result.

For the creation of the software module, a technological scheme was proposed, as shown in Figure 7.

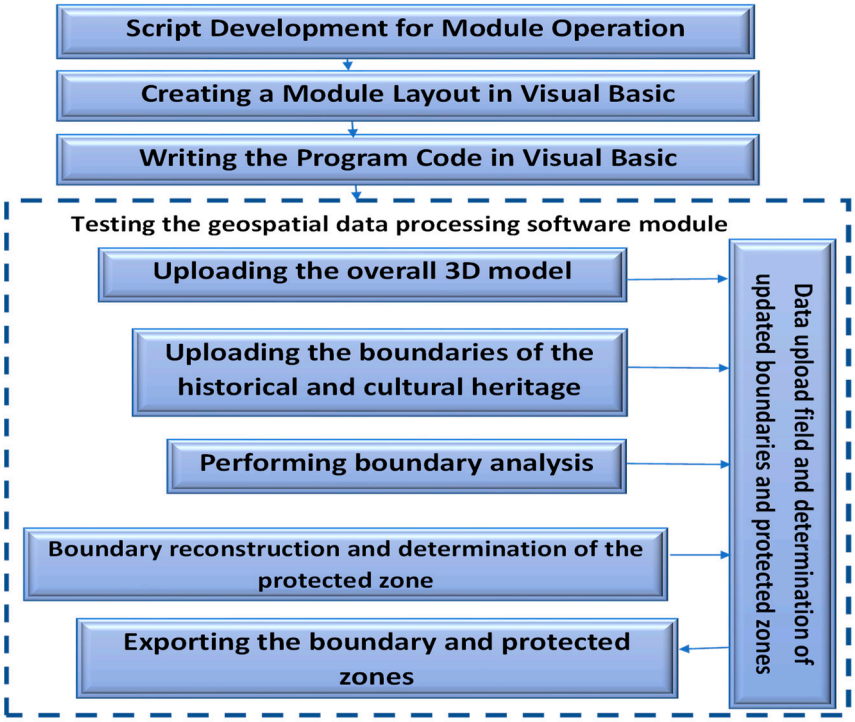


Figure 7. Technological scheme of creating a software module for refining the boundaries of an object and its protective zone.

To automate the described processes, a software module was developed in the VisualBasic programming language for refining the boundaries of historical and cultural heritage sites. Although VisualBasic is less suitable for programming cartographic elements compared to, for example, Python, its advantage lies in its object-oriented nature and full integration with the Windows operating system. By using additional modules available for VisualBasic, we were able to implement the assigned task.

For testing and validation of the created software module, graphical materials on the Lviv Citadel were used in raster and vector formats, namely, Citadel's Cadastral Map in

GeoTIFF format, radarogram of radar scanning of individual areas of interest of the Citadel in GeoTIFF format, vector layer of digitized radarogram anomalies in DXF vector format, and the boundary of the historical and cultural heritage site in DXF vector format.

The program execution started with testing the first functional block "Data Loading". When the command "Load 3D Model" is executed, the GeoTIFF format CAD model of the Citadel is loaded.

Next, we proceed to the next step—loading the radiogram obtained from the ground-penetrating radar survey in GeoTIFF format. Then, commands to load vectorized anomalies based on the radiograms of ground-penetrating radar survey are executed in DXF vector exchange format.

3. Results

The research goals of this paper are demonstrated through a study of the historical and cultural heritage object, the Citadel defensive complex located in Lviv, where the Stalag-328 prisoner-of-war concentration camp was situated during World War II.

Using the obtained interferograms generated from 36 satellite images acquired from the Sentinel-1 satellite over three years from 2020 to 2022, we were able to identify the extremes of vertical ground displacement in the research area. By discarding the indicators of minimal displacement, only the maximum displacements were considered. There were 24 points identified with such displacements. The range of vertical ground displacement at these points varies from 17 to 36 cm. Additional investigations led to the exclusion of five points located within the object's territory in the built-up area. It was hypothesized that the vertical displacements in the built-up area may have occurred due to specific repair works.

As previously mentioned, processing of spaceborne radar images from the Sentinel-1 satellite was performed using the SARScape software with the SBAS method. Evaluating the characteristics of the territory of our research object and its relatively small area in the scale of satellite images, a coherence threshold of -22 decibels was chosen for the most precise filtering of noise and insignificant objects. The range of coherence thresholds for the SBAS method can also vary from several decibels to significant values, depending on the specific study and the nature of the data. Typically, the range of coherence thresholds for SBAS can be from -20 to -30 decibels, or even less. The coherence threshold adjustment was performed by a selection method to ensure the best results.

For the SBAS method, an important step is the selection of baseline pairs. Perpendicular baseline pairs were chosen for measuring deformations along two directions, north–south and west–east. This allowed for measurements of deformations in both horizontal directions. Temporal baseline pairs were selected between pairs of radar images as of January 2020 and December 2020, and January 2021 and December 2021, to cover the desired time period. This allowed for considering the dynamics of deformations of the Earth's surface during the selected time interval, which ranged from -0.7 to -10 cm/year over the selected time period.

It is emphasized that the research was conducted over a three-year period during which centimeter-scale subsidence was recorded, but it is not guaranteed that the average indicators were the same as in previous years. Most likely they were not, as the territory of the object has largely remained unchanged over the past decade.

In the SBAS method for processing radar images from the Sentinel-1 satellite, both descending and ascending geometries can be used. In the case of descending geometry, the same radar satellite is used to obtain both images used in pairs for interferometric analysis. The advantage of such geometry is that images obtained from the same radar satellite have minimal geometry differences, which can improve the quality of interferograms and reduce processing time, while the disadvantage is the limited availability of data, as this depends on the passage of the satellite. In our case, this geometry was used because all images were taken from the Sentinel-1 satellite at monthly intervals.

With regards ascending geometry, in this case, images obtained by different radar satellites (for example, two Sentinel-1 satellites) are used to create image pairs. Its advan-

tages include increasing the available data, as images obtained by different satellites and at different times can be used, while its disadvantages include the possibility of differences in image geometry, which can affect the quality of interferograms and require additional computations for correction.

For obtaining vertical displacements, Line-of-Sight (LOS) estimates obtained from radar images are typically used. Transforming LOS estimates into vertical displacements usually requires additional data on topography and models of spatial distribution of velocity variations. These data are used to correct geometric artifacts and account for effects of horizontal and vertical ground motion. The accuracy of vertical displacement estimates was 0.6 cm as the relief of the object is hilly and it is more difficult to accurately determine vertical displacements.

Furthermore, based on previous research [33], the territory of prisoner shootings and fraternal burials was overlaid onto the modern topographic plan of 2007 at a scale of 1:5000. In these areas, vertical ground displacements may be noticeable due to subsidence even after many years. This is explained by the decomposition of human bodies. Additionally, documentary sources indicate that the Nazis covered human bodies with lime in these areas to accelerate decomposition, which could result in voids forming in the soil. Therefore, the points of extreme vertical displacement were color-coded: green for those falling within the areas of shootings and burials, yellow for those falling on the paved infrastructure likely formed by repair works, and red for those falling on the undeveloped territory. Additionally, the current boundary of the historical and cultural heritage object, represented by a thick black line, is delineated on the plan (Figure 8).

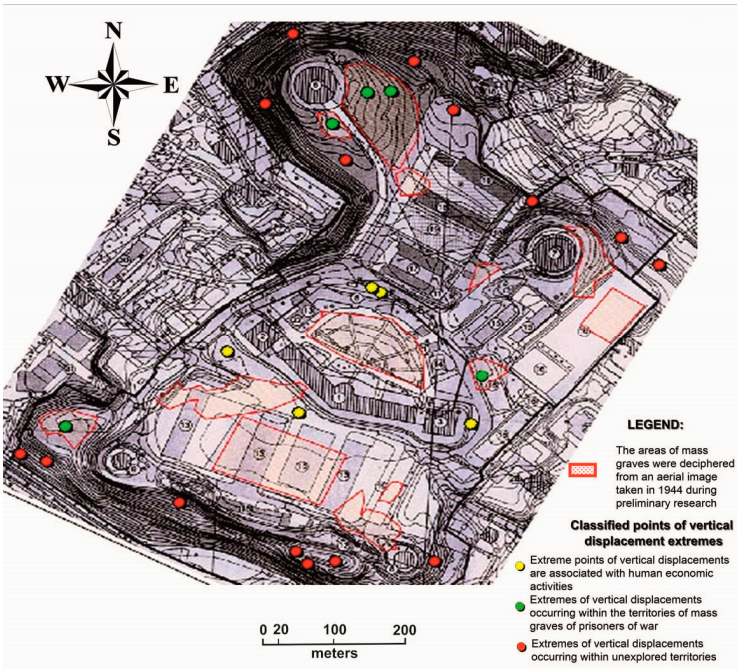


Figure 8. Topographic plan with marked polygonal objects of potential fraternal burials (pink background outlined by red lines) with overlaid points of maximum vertical displacement [34].

The analysis of vertical displacements can reveal potential threats to historical structures, such as precipitation, erosion, soil subsidence, or geodynamic processes. This allows appropriate measures to be taken to prevent potential damage or destruction. Information about vertical displacements can be used for planning restoration work and preserving historical structures. This enables effective restoration measures that take into account the potential impacts of geodynamic processes [35,36]. Maps of vertical displacement serve as documentation of the state of historical structures at a certain period in time. This is important for archiving and monitoring changes over time, as well as for further scientific

research. A map of maximum vertical displacements of the Earth's surface in the territory of the Citadel for the years 2020–2022 is presented in Figure 9.

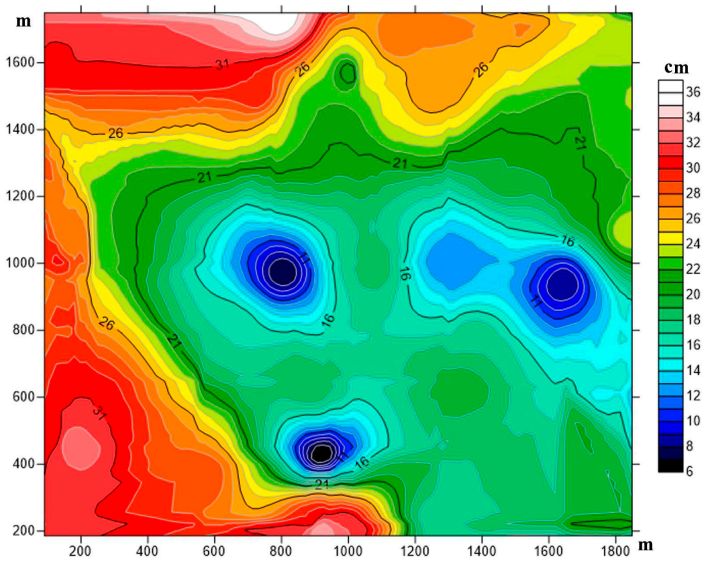


Figure 9. Map of vertical displacements, cm.

Area of Interest (AOI) 1 is a northern tennis court, closest to two smaller barracks. At a depth of approximately 0.3 m (t = 11.88 ns), there is an underground object measuring 20 m × 3 m, which diagonally crosses the tennis court and initially appears on ground-penetrating radar scans at a depth of 0.3 m. This object corresponds precisely to the disturbed ground area visible on the 1944 aerial photograph, and the results match well-defined historical excavations. The edges of the object are particularly well-defined closest to the southwest corner of the tennis court and extend beyond the surveyed area.

The central cross-section of the object has less defined edges throughout its depth, possibly resulting from soil disturbance during the construction of the tennis courts (Figure 10). At a depth of approximately 0.7 m (t = 14.38 ns), the clarity of the sides decreases, and additional features are observed within the main object. These may be reflections from objects within the excavation boundaries, but they are not observed along the entire length of the object and are notably absent where excavations may have occurred previously. Reflections from the northern edge of the object begin to lose clarity at a depth of about 0.8 m (t = 15.63 ns), unlike the southern side, which remains clear at a depth of about 0.93 m (t = 18.44 ns). The object is not visible at depths exceeding 1.1 m (t = 22.1 ns).

Figure 11 illustrates the interval of object AOI1 at a depth of approximately 0.68 m (t = 13.75 ns). Attention should be drawn to the darker visualization parts (higher amplitude) on the left side in the center of the object, indicating a possible disturbance that may have occurred during the construction of the tennis courts.

The AOI2 area, measuring 5 m by 10 m, was surveyed. The results show that the eastern edge of the excavation is outside the established boundary of the object, but based on visual markers, it can be concluded that it does not extend more than 4 m beyond the northeastern boundary. The scanning interval of the profile at t = 10.94 ns, corresponding to an estimated depth of 0.54 m, is oriented differently from what is depicted in Figure 12, the upper edge of which turns out to be the northeastern boundary.

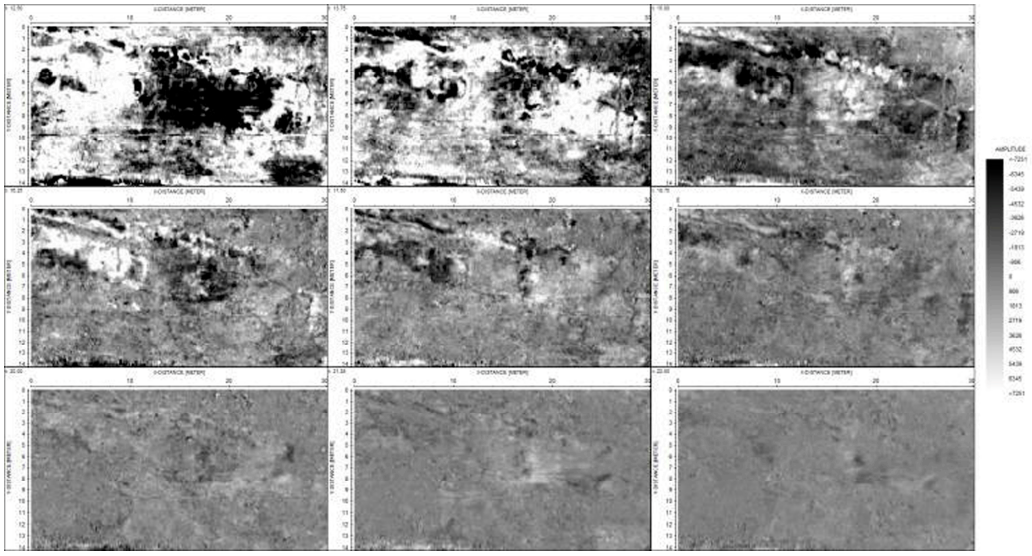


Figure 10. Citadel AOI1-GPR time slices.

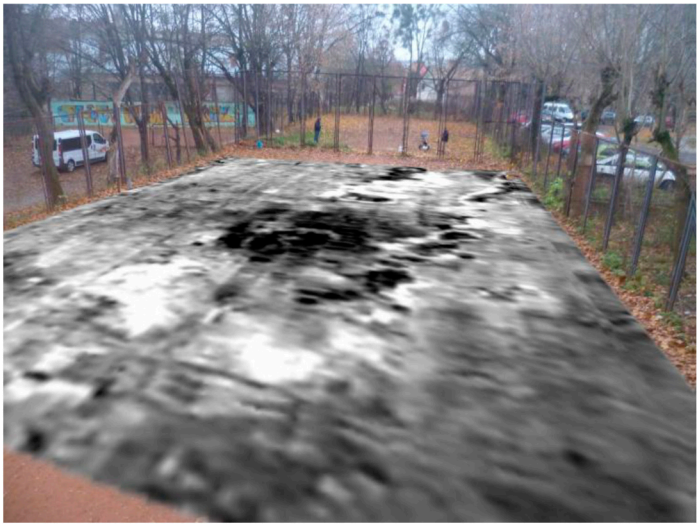


Figure 11. Citadel—an overlay of radargram on modern locality.

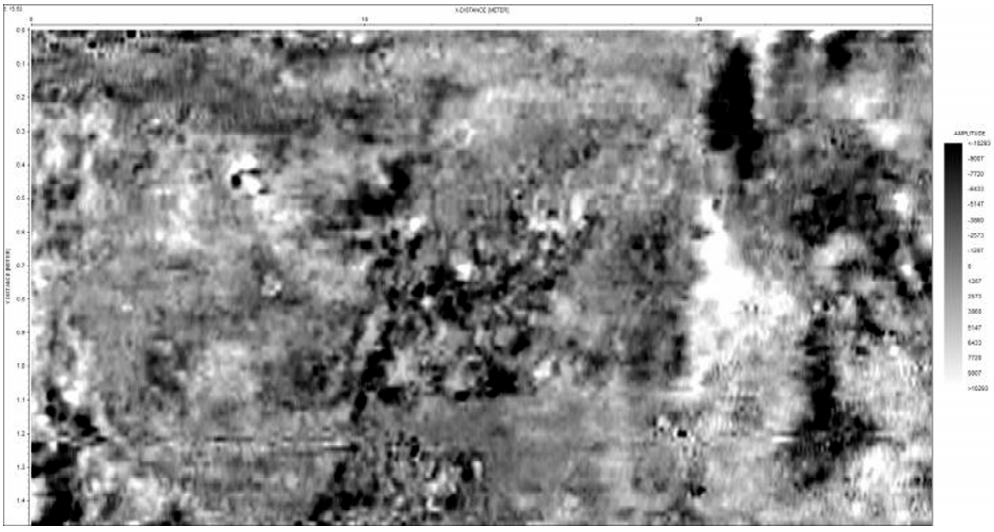


Figure 12. Citadel AOI2—scanogram of the ground-penetrating radar at t = 15.63 ns.

Figure 12 illustrates the interval of the object at a depth of approximately 0.78 m (t = 15.63 ns). A rectangular object can be seen below the center of the image. The soil outside the 1944 fence is located on the right side.

Due to difficulties in data collection, further analysis of this anomaly proves challenging. This anomaly is difficult to identify at various depths using the profile scanning intervals, but it can be identified through multiple cross-sections.

Using the newly obtained data from radar and ground-penetrating radar surveys, the boundaries of the historical and cultural heritage object, established to date by the Ministry of Culture of Ukraine and recognized as the official cadastral boundaries of the object entered into the Public Cadastral Map of Ukraine, have been overlaid onto the modern topographic map from 2007, with a scale of 1:1000. Additionally, adjustments were made to the boundaries in light of the newly discovered underground artifacts (Figure 13).

For the validation of the conceptual model for refining the boundaries of historical and cultural heritage sites and establishing protection zones around these sites, a software module has been developed and programmed. This module processes the synthetic aperture radar (SAR) data of the surface part and the ground-penetrating radar (GPR) profiles of the underground part of the object [37,38]. The main challenge in developing this software module was to mathematically integrate the results obtained from SAR and GPR.

Mathematical reconciliation of radar and ground-penetrating radar (GPR) data can be achieved using various data processing methods, including filtering and signal processing techniques. One approach to reconciling the results involves utilizing filtering algorithms such as the Kalman filter. This method relies on computing the system state estimation based on processed information from all sources and modeling the system using stochastic differential equations. Another approach to reconciling the data involves using signal processing algorithms like correlation analysis. This method is based on comparing signals obtained from different sources and determining the degree of their correspondence. Additionally, other mathematical methods such as principal component analysis, classification methods, and pattern recognition can be employed to reconcile the data processing results.

Regardless of the approach, when reconciling the results of radar and GPR data processing, it is essential to consider the characteristics of each method and data source and ensure the quality and accuracy of data processing.

In fact, the dataset loaded in the window in Figure 14 is final for analysis, and we can proceed to the next functional block. The first command executed in the second block is "Boundary Analysis", and its execution is hidden, with the result being loaded into the computer's memory—that is, after executing this command, the picture inside the window remains unchanged. This command performs an overlay analysis of the loaded data, after which the module determines whether all additional elements fit within the existing object boundary. If so, the next commands are unnecessary. If not, the software rebuilds the boundary according to the newly identified elements [39–43].

The next step is executing the command for boundary reconstruction (Figure 15), as a result of which the program visualizes the outcome of the previous step from its memory in the data field. After the reconstruction of the object's boundaries according to the new elements, the protective zone of the cultural heritage object is constructed (Figure 16). A protective zone can be established with a radius of 100, 200, or 300 m. The width of the protective zone depends on the development of the area and is selected by the user when using the module.

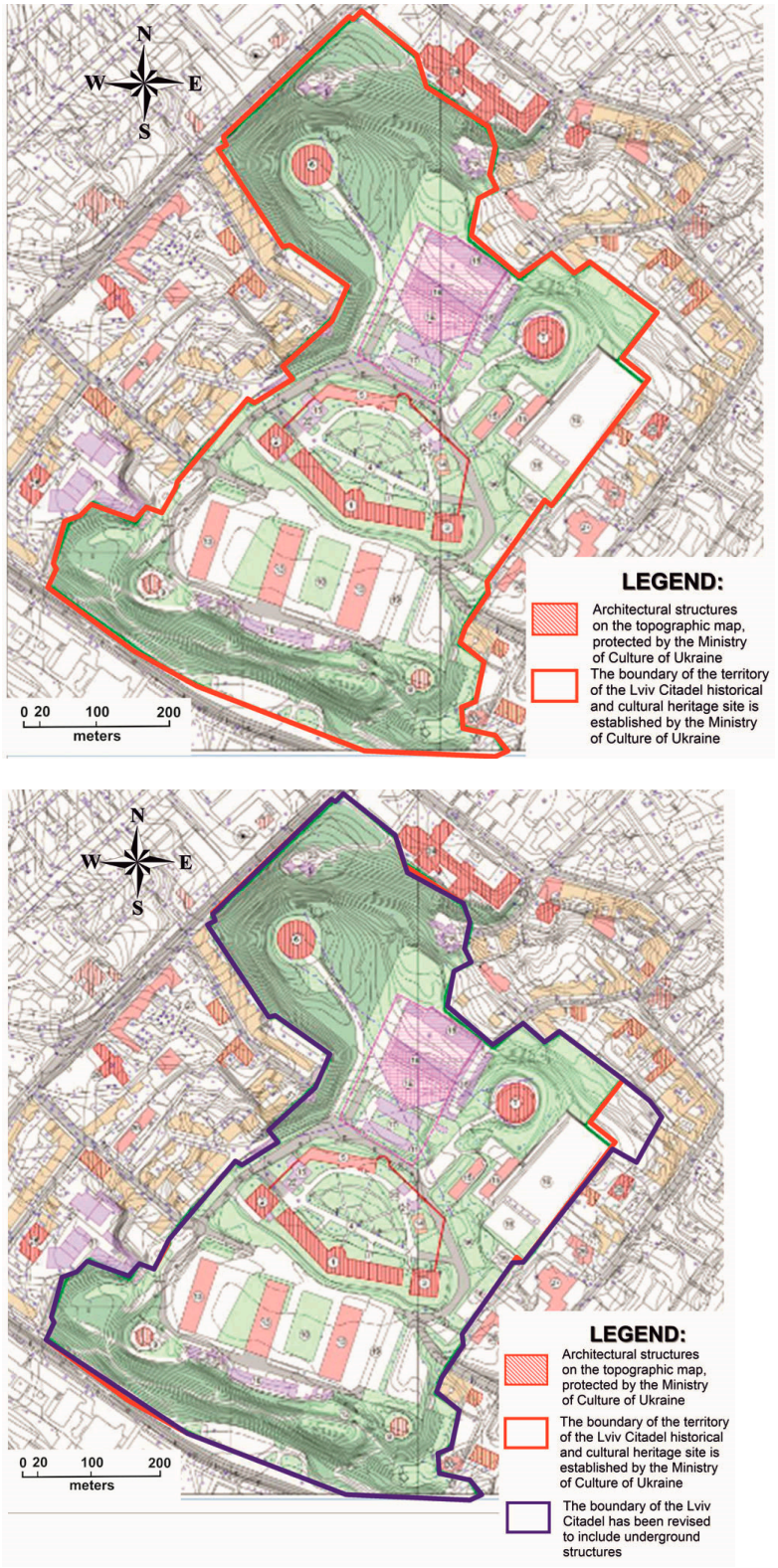


Figure 13. The boundary of the historical and cultural heritage site established by the Ministry of Culture of Ukraine based on archival cartographic and aerial materials (red color), and the adjusted boundary considering radar and ground-penetrating radar surveys (blue color).

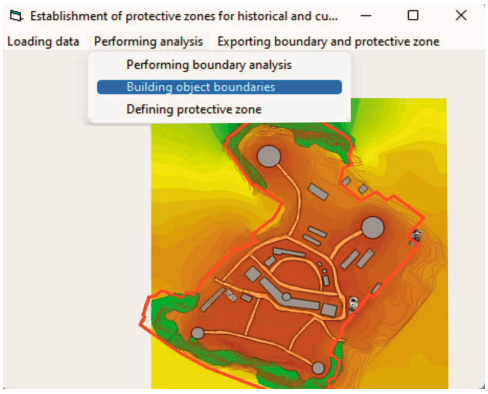


Figure 14. Loading all input data into the module's workspace.

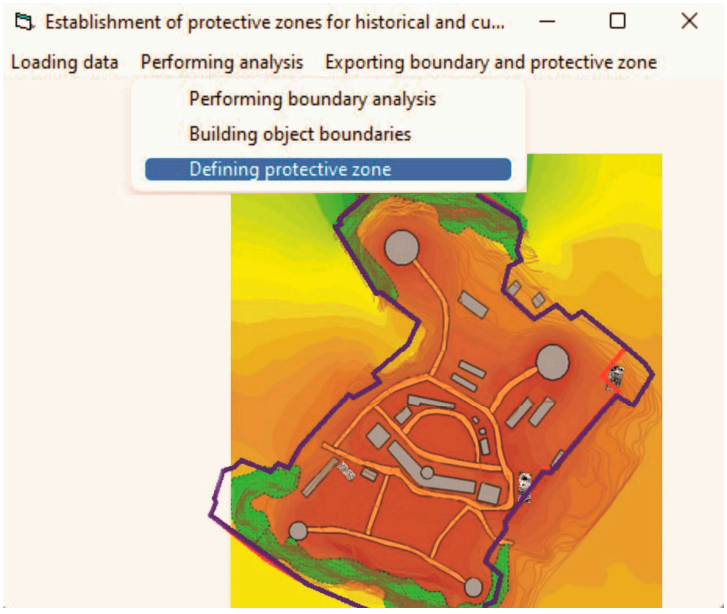


Figure 15. Reconstruction of the object's boundary according to newly discovered data.

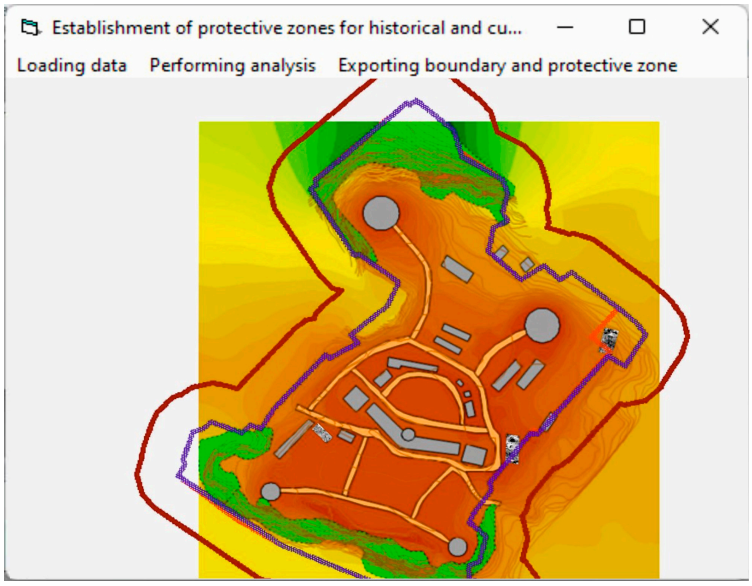


Figure 16. Construction of the protective zone around the corrected boundary of the object.

The result of the module execution is the reconstructed updated boundary of the object of historical and cultural heritage with an automatically generated protective zone. This result can then be exported to the exchange vector format DXF and opened in any geographic information system or CAD system for further work.

It is worth noting that this module is advisable to apply to already registered objects of cultural heritage based on the centroids of polygons when there is a need for directly refining the boundaries of the object itself.

The automatically constructed refined boundary of the object (the line is marked in blue in Figures 15 and 16), after determining the underground elements with GPR, coincides with the previously established boundary overall and differs only in the northeastern part where the GPR was conducted. The software module automatically constructs a line at a distance of 15 m from the newly discovered underground elements located within the old boundaries of the object.

4. Discussion

Many Non-Destructive Techniques (NDT) can be fused into monitoring selected infrastructure [44] or searching objects of interest. In our approach, InSAR data are used initially to detect locations for more detailed analyses with more detailed technology (GPR). Such an approach was presented in [45] where a large dataset of SAR images from both the Sentinel 1A and COSMO-SkyMed and GPR data was tested for long railway line inventory. In this case, data sets were collected with both techniques for whole corridor mapping but, similarly to our approach, spots detected as having subsidence were deeply analyzed using GPR observations. In some approaches, those two radar techniques can be complementary to each other. In some examples, SAR and GPR can be used in one investigation but are used and analyzed separately [46] in a common investigation, which can provide additive benefits. An example of such methodology was presented in [47], where it was stated that despite GPR and PS-InSAR methodologies both collecting a considerable amount of data, outcomes are incomplete if considered singularly. The last example of an approach in which the integration of these two radar technologies can be related somehow is using one technology in the verification of another. In some examples, SAR—as technology providing lower-resolution data—can be verified with GPR that is collected onsite with remote sensing techniques [34]. Considering cultural heritage, the role of radar techniques and their integration has grown rapidly in recent years [48]. Such integration always requires, first of all, appropriate georeferencing in the common reference frame, which gives the possibility of integrating layers in the geographic information system.

5. Conclusions

The refinement of boundaries for immovable historical and cultural heritage objects and the determination of their protective zones using remote sensing methods represent crucial steps in preserving and safeguarding these invaluable assets. Through the application of remote sensing techniques, such as satellite imagery and ground-penetrating radar, precise boundaries can be delineated, allowing for effective management and conservation efforts. This conceptual approach not only aids in the identification of potential threats to heritage sites but also facilitates the planning of archaeological excavations and scientific research initiatives aimed at further understanding the historical and cultural significance of these objects. By integrating remote sensing data into the geographical information system, comprehensive models can be developed to guide conservation strategies and mitigate risks associated with urbanization, tourism, and natural disasters. Overall, the utilization of remote sensing methods offers a valuable toolset for enhancing the protection and preservation of immovable historical and cultural heritage objects for future generations.

In this study, conceptual and detailed models are proposed for the study of cultural heritage objects using remote and non-invasive methods, and a technological scheme for their implementation has been developed. Extremes of vertical displacement of the Earth's surface within the territory of the Citadel, an object of cultural heritage in Lviv, were

determined based on interferograms created using the radar interferometry method from 36 Sentinel-1 satellite images spanning from 2020 to 2022. A total of 24 such points were identified.

The obtained extremes of vertical displacement were investigated using ground-penetrating radar imaging. Special attention was paid to two areas where anomalies were observed, one of which lies beyond the currently established boundary of the object.

A software module for refining the boundaries of cultural heritage objects and determining their protective zones has been developed and programmed. Additionally, a technological scheme for implementing the module development process has been provided.

Further research will involve performing aerial laser scanning of the research object, conducting aerial photography using UAVs, and utilizing optical-electronic satellite images to enhance the data, which will be used for automatic analysis of the horizontal and vertical positioning of the object in the developed software module.

Author Contributions: Methodology development: B.C.; writing—original draft: V.H.; writing—review and editing: K.B. All authors have read and agreed to the published version of the manuscript.

Funding: The APC was funded by the Polish National Agency for Academic Exchange within the project "Development of strategic cooperation between Warsaw University of Technology and Lviv Polytechnic National University in the field of geomatics" agreement number BPI/PST/2021/1/00044/U/00001.

Data Availability Statement: Data are unavailable due to privacy and ethical restrictions.

Conflicts of Interest: The authors declare no conflicts of interest. The funders had no role in the design of the study; in the collection, analyses, or interpretation of data; in the writing of the manuscript; or in the decision to publish the results.

References

1. Liu, Y.; Tang, Y.; Jing, L.; Chen, F.; Wang, P. Remote Sensing-Based Dynamic Monitoring of Immovable Cultural Relics, from Environmental Factors to the Protected Cultural Site: A Case Study of the Shunji Bridge. *Sustainability* **2021**, *13*, 6042. [CrossRef]
2. Koeva, M.; Luleva, M.; Maldjanski, P. Integrating Spherical Panoramas and Maps for Visualization of Cultural Heritage Objects Using Virtual Reality Technology. *Sensors* **2017**, *17*, 829. [CrossRef] [PubMed]
3. Moise, C.; Dana Negula, I.; Mihalache, C.E.; Lazar, A.M.; Dedulescu, A.L.; Rustoiu, G.T.; Inel, I.C.; Badea, A. Remote Sensing for Cultural Heritage Assessment and Monitoring: The Case Study of Alba Iulia. *Sustainability* **2021**, *13*, 1406. [CrossRef]
4. Megarry, W.P.; Cooney, G.; Comer, D.C.; Priebe, C.E. Posterior Probability Modeling and Image Classification for Archaeological Site Prospection: Building a Survey Efficacy Model for Identifying Neolithic Felsite Workshops in the Shetland Islands. *Remote Sens.* **2016**, *8*, 529. [CrossRef]
5. Borie, C.; Parcero-Oubiña, C.; Kwon, Y.; Salazar, D.; Flores, C.; Olguín, L.; Andrade, P. Beyond Site Detection: The Role of Satellite Remote Sensing in Analysing Archaeological Problems. A Case Study in Lithic Resource Procurement in the Atacama Desert, Northern Chile. *Remote Sens.* **2019**, *11*, 869. [CrossRef]
6. Tapete, D.; Cigna, F. Appraisal of Opportunities and Perspectives for the Systematic Condition Assessment of Heritage Sites with Copernicus Sentinel-2 High-Resolution Multispectral Imagery. *Remote Sens.* **2018**, *10*, 561. [CrossRef]
7. Bai, X.; Du, P.; Guo, S.; Zhang, P.; Lin, C.; Tang, P.; Zhang, C. Monitoring Land Cover Change and Disturbance of the Mount Wutai World Cultural Landscape Heritage Protected Area, Based on Remote Sensing Time-Series Images from 1987 to 2018. *Remote Sens.* **2019**, *11*, 1332. [CrossRef]
8. Elfadaly, A.; Shamseldein, A.; Lasaponara, R. Cultural Heritage Management Using Remote Sensing Data and GIS Techniques around the Archaeological Area of Ancient Jeddah in Jeddah City, Saudi Arabia. *Sustainability* **2020**, *12*, 240. [CrossRef]
9. Tang, P.; Chen, F.; Zhu, X.; Zhou, W. Monitoring Cultural Heritage Sites with Advanced Multi-Temporal InSAR Technique: The Case Study of the Summer Palace. *Remote Sens.* **2016**, *8*, 432. [CrossRef]
10. Zhou, W.; Chen, F.; Guo, H. Differential Radar Interferometry for Structural and Ground Deformation Monitoring: A New Tool for the Conservation and Sustainability of Cultural Heritage Sites. *Sustainability* **2015**, *7*, 1712–1729. [CrossRef]
11. Cigna, F.; Lasaponara, R.; Masini, N.; Milillo, P.; Tapete, D. Persistent Scatterer Interferometry Processing of COSMO-SkyMed StripMap HIMAGE Time Series to Depict Deformation of the Historic Centre of Rome, Italy. *Remote Sens.* **2014**, *6*, 12593–12618. [CrossRef]
12. Lasaponara, R.; Elfadaly, A.; Attia, W. Low cost space technologies for operational change detection monitoring around the archaeological area of Esna-Egypt. In *Lecture Notes in Computer Science, Proceedings of the Computational Science and Its Applications–ICCSA 2016, Beijing, China, 4–7 July 2016*; Gervasi, O., Murgante, B., Misra, S., Rocha, A.M.A.C., Torre, C.M., Taniar, D., Apduhan, B.O., Stankova, E., Wang, S., Eds.; Springer: Cham, Switzerland, 2016; Volume 9787.

13. Tofani, V.; Raspini, F.; Catani, F.; Casagli, N. Persistent Scatterer Interferometry (PSI) Technique for Landslide Characterization and Monitoring. *Remote Sens.* **2013**, *5*, 1045–1065. [CrossRef]
14. Drahor, M.G. A review of integrated geophysical investigations from archaeological and cultural sites under encroaching urbanisation in Izmir, Turkey. *Phys. Chem. Earth* **2011**, *36*, 1294–1309. [CrossRef]
15. Elfadaly, A.; Attia, W.; Qelichi, M.M.; Murgante, B.; Lasaponara, R. Management of Cultural Heritage Sites Using Remote Sensing Indices and Spatial Analysis Techniques. *Surv. Geophys.* **2018**, *39*, 1347–1377. [CrossRef]
16. Beraldin, J.A.; Picard, M.; El-Hakim, S.F.; Godin, G.; Valzano, V.; Bandiera, A. Combining 3D technologies for cultural heritage interpretation and entertainment. In *Electronic Imaging*; International Society for Optics and Photonics: Bellingham, WA, USA, 2005; pp. 108–118.
17. Remondino, F.; Girardi, S.; Gonzo, L.; Rizzi, A. Multiresolution modeling of complex and detailed cultural heritage. In Proceedings of the 9th International Symposium on Virtual Reality, Archaeology and Cultural Heritage (VAST 2008), Braga, Portugal, 2–5 December 2008; pp. 1–8.
18. Remondino, F.; Rizzi, A.; Agugiaro, G.; Girardi, S.; De Amicis, R.; Magliocchetti, D.; Girardi, G.; Baratti, G. Geomatics and geoinformatics for digital 3D documentation, fruition and valorization of cultural heritage. In Proceedings of the EUROMED 2010 Workshop on Museum Futures: Emerging Technological and Social Paradigms, Lemessos, Cyprus, 8–13 November 2010; pp. 8–13.
19. Meyer, D.; Fraijo, E.; Lo, E.; Rissolo, D.; Kuester, F. Optimizing UAV systems for rapid survey and reconstruction of large scale cultural heritage sites. In Proceedings of the Digital Heritage, Granada, Spain, 28 September–2 October 2015.
20. Themistocleous, K.; Ioannides, M.; Agapiou, A.; Hadjimitsis, D.G. The methodology of documenting cultural heritage sites using photogrammetry, UAV, and 3D printing techniques: The case study of Asinou church in Cyprus. In Proceedings of the Third International Conference on Remote Sensing and Geoinformation of the Environment, Paphos, Cyprus, 16–19 March 2015.
21. Rinaudo, F.; Chiabrando, F.; Nex, F.; Piatti, D. New instruments and technologies for cultural heritage survey: Full integration between point clouds and digital photogrammetry. In *Digital Heritage*; Springer: Berlin/Heidelberg, Germany, 2010; pp. 56–70.
22. Gleich, D. Detection of Wet Zones Within a Hydro-Power Plant's Canal Using SAR and GPR Data. *IEEE J. Sel. Top. Appl. Earth Obs. Remote Sens.* **2013**, *6*, 1864–1878. [CrossRef]
23. Zych, M. Methods of Achieving Good GPR Image Resolution Using Focused SAR Processing. *Int. J. Electron. Telecommun.* **2011**, *57*, 49–54. [CrossRef]
24. Mostafa, M.A.; Samir, M.; Hussein, K.; Kamel, H. SAR Processing for Buried Objects Detection using GPR. *J. Multidiscip. Eng. Sci. Technol. (JMEST)* **2016**, *3*, 2458–9403.
25. Nottebaere, M.; Ardekani, M.R.; Lambot Sand Neyt, X. SAR-image derived soil moisture enhancement using GPR data. In Proceedings of the 15th International Conference on Ground Penetrating Radar, Brussels, Belgium, 30 June–4 July 2014; pp. 223–226. [CrossRef]
26. Lisini, G.; Tison, C.; Tupin, F.; Gamba, P. Feature fusion to improve road network extraction in high-resolution SAR images. *IEEE Geosci. Remote Sens. Lett.* **2006**, *3*, 217–221. [CrossRef]
27. Figueiredo, R.; Romo, X.; Paupério, E. Flood risk assessment of cultural heritage at large spatial scales: Framework and application to mainland Portugal. *J. Cult. Herit.* **2020**, *43*, 163–174. [CrossRef]
28. Luo, L.; Wang, X.; Guo, H.; Lasaponara, R.; Zong, X.; Masini, N.; Wang, G.; Shi, P.; Khatteli, H.; Chen, F.; et al. Airborne and spaceborne remote sensing for archaeological and cultural heritage applications: A review of the century (1907–2017). *Remote Sens. Environ.* **2019**, *232*, 232. [CrossRef]
29. Luo, L.; Wang, X.; Lasaponara, R.; Xiang, B.; Zhen, J.; Zhu, L.; Yang, R.; Liu, D.; Liu, C. Auto-extraction of linear archaeological traces of Tuntian Irrigation Canals in Miran Site (China) from Gaofen-1 satellite imagery. *Remote Sens.* **2018**, *10*, 718. [CrossRef]
30. Lopes, A.S.; Macedo, D.V.; Brito, A.; Furtado, V. Assessment of urban cultural-heritage protection zones using a co-visibilityanalysis tool. *Comput. Environ. Urban Syst.* **2019**, *76*, 139–149. [CrossRef]
31. Choi, Y.; Yang, Y.J.; Sohn, H.G. Resilient cultural heritage through digital cultural heritage cube: Two cases in South Korea. *J. Cult. Herit.* **2021**, *48*, 36–44. [CrossRef]
32. Banerjee, R.; Srivastava, P.K. Reconstruction of contested landscape: Detecting land cover transformation hosting cultural heritage sites from Central India using remote sensing. *Land Use Policy* **2013**, *34*, 193–203. [CrossRef]
33. Chetverikov, B.; Babiy, L. Determination of boundaries of ancient burial places using the archived aerial and cartographic materials. *Mod. Achiev. Geod. Sci. Ind.* **2016**, *1*, 111–114.
34. Chetverikov, B.; Protsyk, M. Analysis of vertical ground displacements of the Lviv Citadel territory based on radar survey data. In Proceedings of the International Conference of Young Professionals "GeoTerrace-2023", Lviv, Ukraine, 2–4 October 2023.
35. Agapiou, A.; Lysandrou, V.; Alexakis, D.D.; Themistocleous, K.; Cuca, B.; Argyriou, A.; Sarris, A.; Hadjimitsis, D.G. Cultural heritage management and monitoring using remote sensing data and GIS: The case study of Paphos area, Cyprus. *Comput. Environ. Urban Syst.* **2015**, *54*, 230–239. [CrossRef]
36. Aminzadeh, B.; Samani, F. Identifying the boundaries of the historical site of Persepolis using remote sensing. *Remote Sens. Environ.* **2006**, *102*, 52–62. [CrossRef]
37. Tsiafaki, D.; Michailidou, N. Benefits and problems through the application of 3d technologies in archaeology: Recording, visualisation, representation and reconstruction. *Sci. Cult.* **2015**, *1*, 37–45.

38. Hatzopoulos, J.N.; Stefanakis, D.; Georgopoulos, A.; Tapinaki, S.; Pantelis, V.; Liritzis, I. Use of various surveying technologies to 3d digital mapping and modelling of cultural heritage structures for maintenance and restoration purposes: The tholos in DELPHI, GREECE. *Mediterr. Archaeol. Archaeom.* **2017**, *17*, 311–336.
39. Roenholm, P.; Honkavaara, E.; Litkey, P.; Hyyppä, H.; Hyyppä, J. Integration of laser scanning and photogrammetry. In Proceedings of the ISPRS Workshop on Laser Scanning 2007 and SilviLaser 2007, Espoo, Finland, 12–14 September 2007; pp. 355–362.
40. Fangi, G.; Clini, P.; Fiori, F. Simple and quick digital technique for the safeguard of Cultural Heritage. The Rustem Pasha Mosque in Istanbul. In Proceedings of the Digital Media and Its Application in Cultural Heritage, Amman, Jordan, 5–6 November 2008; pp. 209–217.
41. Kersten, T.P.; Lindstaedt, M. Image-based low-cost systems for automatic 3D recording and modelling of archaeological finds and objects. In *Progress in Cultural Heritage Preservation*; Springer: Berlin/Heidelberg, Germany, 2012; pp. 1–10.
42. García-Gago, J.; González-Aguilera, D.; Gómez-Lahoz, J.; San José-Alonso, J.I. A photogrammetric and computer vision-based approach for automated 3D architectural modeling and its typological analysis. *Remote Sens.* **2014**, *6*, 5671–5691. [CrossRef]
43. Andretta, M.; Coppola, F.; Modelli, A.; Santopuoli, N.; Seccia, L. Proposal for a new environmental risk assessment methodology in cultural heritage protection. *J. Cult. Herit.* **2017**, *23*, 22–32. [CrossRef]
44. Koohmishi, M.; Kaewunruen, S.; Chang, L.; Guo, Y. Advancing railway track health monitoring: Integrating GPR, InSAR and machine learning for enhanced asset management. *Autom. Constr.* **2024**, *162*, 105378. [CrossRef]
45. Bianchini Ciampoli, L.; Gagliardi, V.; Clementini, C.; Latini, D.; Del Frate, F.; Benedetto, A. Transport infrastructure monitoring by InSAR and GPR data fusion. *Surv. Geophys.* **2020**, *41*, 371–394. [CrossRef]
46. D'Amico, F.; Gagliardi, V.; Ciampoli, L.B.; Tosti, F. Integration of InSAR and GPR techniques for monitoring transition areas in railway bridges. *NDT E Int.* **2020**, *115*, 102291. [CrossRef]
47. Chen, F.; Guo, H.; Tapete, D.; Cigna, F.; Piro, S.; Lasaponara, R.; Masini, N. The role of imaging radar in cultural heritage: From technologies to applications. *Int. J. Appl. Earth Obs. Geoinf.* **2022**, *112*, 102907. [CrossRef]
48. Jiang, A.H.; Chen, F.L.; Tang, P.P.; Liu, G.L.; Liu, W.K.; Wang, H.C.; Lu, X.; Zhao, X.L. Radar remote sensing for archaeology in Hangu Frontier Pass in Xin'an, China. In *IOP Conference Series: Earth and Environmental Science*; IOP Publishing: Bristol, UK, 2017; Volume 57, p. 012031.

Disclaimer/Publisher's Note: The statements, opinions and data contained in all publications are solely those of the individual author(s) and contributor(s) and not of MDPI and/or the editor(s). MDPI and/or the editor(s) disclaim responsibility for any injury to people or property resulting from any ideas, methods, instructions or products referred to in the content.